MODELING PROPAGATION OF COHERENT OPTICAL PULSES THROUGH MOLECULAR VAPOR

Bruce W. Shore
Lawrence Livermore National Laboratory, Livermore, CA 94550

Joseph H. Eberly
Department of Physics and Astronomy
University of Rochester, Rochester, NY 14627

UCRL--87078

DE82 013793

Abstract

We describe results of modeling the mutual coupling of coherent molecular response and coherent optical pulses during propagation. We treat the propagation numerically, with particular emphasis on both continuum and discrete behavior associated with the quasicontinuum model.

Introduction

Traditional descriptions of radiation transport in vapors assume that absorption of radiation occurs in accord with a linear Einstein rate equation. That is, the rate of change in molecular level population is assumed directly proportional to the molecular population inversion. By the same token, the absorption process is assumed to deplete the radiant intensity in accord with the linear Beer-Lambert law of attenuation: the rate of depletion of intensity with distance is locally proportional to the intensity.

The propagation of intense short-duration radiation pulses through a vapor can differ markedly from the classical Beer-Lambert exponential attenuation, particularly when the pulse carrier frequency matches a Bohr transition frequency from the ground state of the vapor: pulse reshaping, pulse breakup into solitons, and self-induced transparency are amongst the phenomena now known to occur in simple two-level excitation.[1,2] It has also been suggested that appropriate conditions may lead to excitation enhancement through propagation.[3-5] We expect that further novel effects remain to be discovered as we explore more elaborate excitation systems.[6] Today we describe some of our steps toward understanding resonant propagation through molecular vapor.

The Equations

In our work we neglect incoherent relaxation processes, so that the excitation dynamics is governed by the time-dependent Schrödinger equation appropriate to electric-dipole excitation by the electric field E. The resulting state vector Ψ, used to calculate the expectation value of the dipole moment d, averaged over any statistical distribution of initial conditions, yields the macroscopic polarization P appropriate to molecular density $\mathcal{N}$. This polarization acts, in turn, as a source term for the Maxwell equations appropriate to radiation--the inhomogeneous wave equation for the electric field. Figure 1 exhibits these coupled equations.

Maxwell for E

$$\left[\nabla^2 - \frac{1}{c^2}\frac{\partial^2}{\partial t^2}\right]\vec{E} = \frac{4\pi}{c^2}\frac{\partial^2}{\partial t^2}\vec{P}$$

Polarization

$$\vec{P} = \mathcal{N}\left\{\langle\Psi|\vec{d}|\Psi\rangle\right\}_{av}$$

Schrödinger for Ψ

$$i\hbar\frac{\partial}{\partial t}\Psi = (H^\circ - \vec{d}\cdot\vec{E})\,\Psi$$

FIG. 1. Maxwell-Schrödinger equations.

MSW

Expansions:

$$\vec{E} = \mathcal{R}e \sum_{\lambda} \frac{\hbar}{ea_0} \vec{F}_\lambda e^{-i(\omega_\lambda t - k_\lambda z)}$$

$$\Psi = \sum_m \psi_m C_m e^{i\phi_m t} \quad \text{with} \quad P_m = |C_m|^2$$

Coupled equations for F_λ and C_m

$$\left[\frac{\partial}{\partial z} - \frac{1}{c}\frac{\partial}{\partial t}\right] F_\lambda = i g_\lambda \sum 2 D^\lambda_{mn} \left\{C^*_n C_m\right\}_{av} \quad \text{with} \begin{cases} n < m \\ \omega_{nm} = \omega_\lambda \end{cases}$$

$$\left[\frac{\partial}{\partial t} + i\Delta_n + \frac{1}{2}\gamma_n\right] C_n = i \sum_m C_m \begin{cases} \frac{1}{2} D^\lambda_{nm} F^\lambda & \text{for } n < m \\ \frac{1}{2} (D^\lambda_{nm} F^\lambda)^* & n > m \end{cases}$$

Distance scale: $x_\lambda = g_\lambda z \equiv \left[2\pi \frac{e^2 a_0^2}{\hbar c} \cdot \mathcal{N} \cdot \omega_\lambda\right] \cdot z$

FIG. 2. Maxwell-Schrödinger equations.

Following conventional approaches, we express the electric field as a combination of slowly varying plane-wave envelopes F_λ and carrier frequencies $\omega_\lambda = k_\lambda/c$. We idealize the molecules as systems comprising relatively few discrete levels linked by near-resonant excitation--the N-level approximation embodied in the expansion of Ψ in a basis of N states ψ_m. The probability of observing population in level m is P_m and the phases ϕ_m are chosen for subsequent convenience.

These two expansions, shown in Fig. 2, taken with the slowly varying envelope approximation for F_λ and the rotating wave approximation for C_m, lead to a set of of coupled non-linear partial differential equations, the plane-wave Maxwell-Schrödinger equations[1] shown in Fig. 2. Here the summation proceeds over those transitions $n < m$ for which the Bohr frequency ω_{nm} is resonant with the mode frequency ω_λ. The gain parameter g_λ provides the basic distance scale $x_\lambda = g_\lambda z$ of Icsevgi and Lamb.[7]

Although analytical solutions are possible for special conditions of two level atoms, we solve the equations numerically, following the general approach of Icsevgi and Lamb.[7]

Basic Questions

Soon after we constructed the necessary computer codes to solve the coupled Maxwell-Schrödinger equations (2.7)-(2.8), Makarov, Cantrell, and Louisell,[3] suggested that a sharply initiated (square wave) pulse, off resonance for a two-level atom, might through propagation induce complete population inversion. Subsequently, Berman and Zaslavsky[5] suggested population enhancement might occur if the excited system were an anharmonic oscillator.

We found that in neither two-level nor anharmonic systems did propagation significantly enhance excitation.[8,9] But our studies did raise other questions, which we have begun investigating:

a. How does the addition of non-resonant levels alter the familiar two-level behavior?
b. Are there special configurations of energy levels which, with propagation, will enhance population transfer from the ground level into excited levels?
c. Under what conditions is excitation coherence relevant?
d. What are the essential features of pulse propagation through a collisionless molecular vapor?
e. What is the minimum configuration of energy levels needed to model accurately the essence of multi-level molecular absorption?

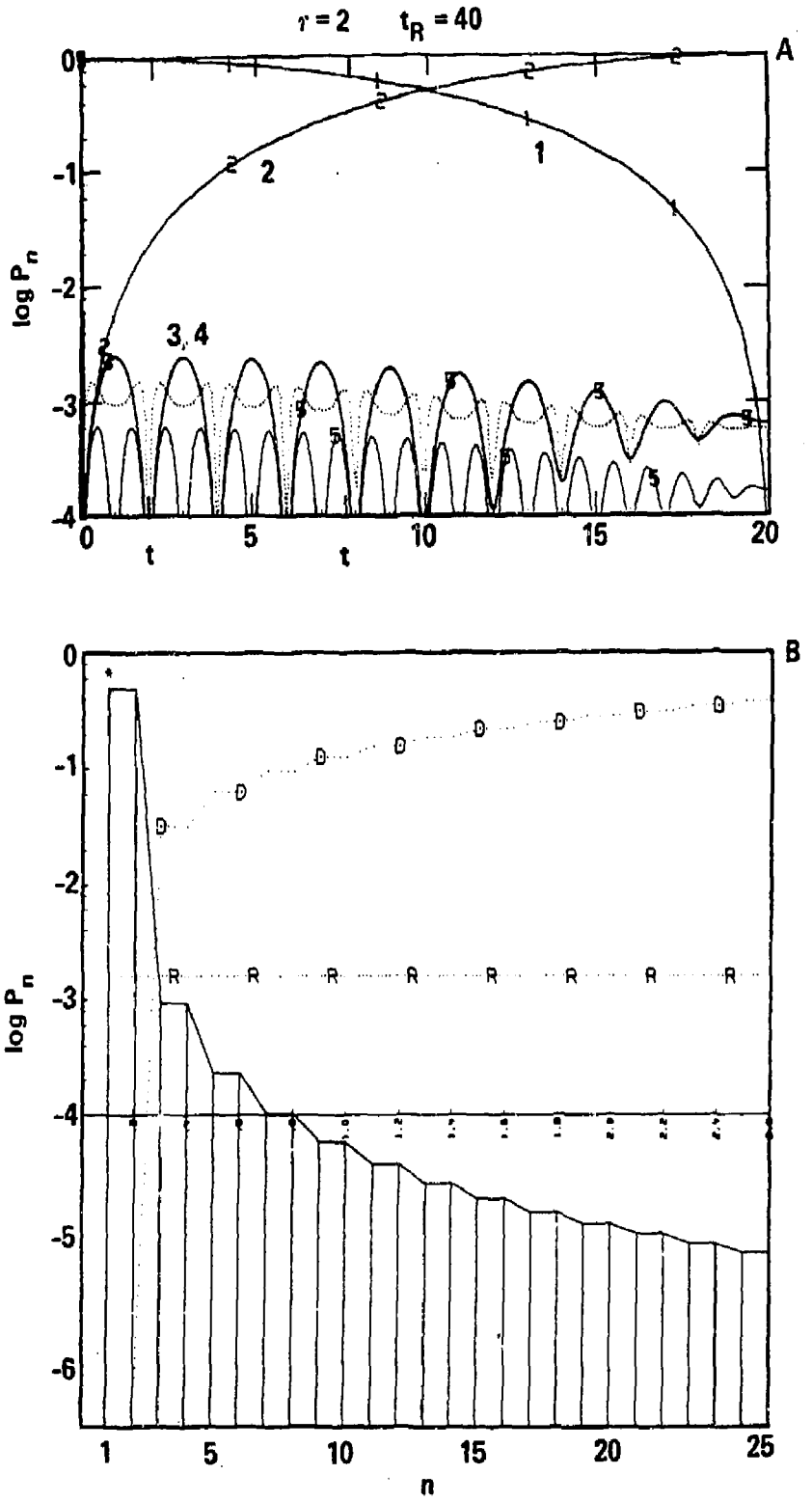

FIG. 4. Weak field quasicontinuum.

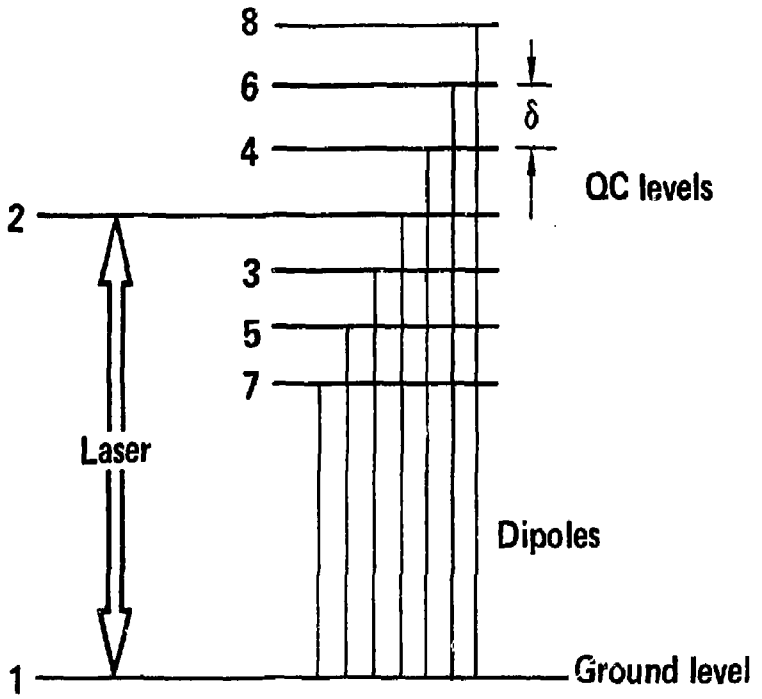

FIG. 3. Quasicontinuum model.

The Quasicontinuum Model

Many discussions of laser-induced molecular excitation[10] recognize that in polyatomic molecules the energy levels become increasingly dense, even for low energies, so that the molecule can behave toward photon absorption as though the molecular energy levels formed a nearly continuous distribution--the so-called quasicontinuum (QC). Because the quasicontinuum is so often invoked to explain features of laser-induced molecular excitation, it is important to understand both the underlying physics of optically thin excitation of QC as well as the QC effect on propagation. We shall describe some numerical studies aimed at clarifying the nature of optically thin excitation of quasicontinua.

Figure 3 shows the simplified QC model we considered:[11] an N-level quasicontinuum (N = 7 here) whose nondegenerate equally-spaced levels are all linked by equal dipole moments to the ground level. A pulse laser with carrier frequency tuned to the central level of the QC (level 2) excites the molecule.

We let the QC levels be evenly spaced with angular frequency separation δ and we let the dipole moments d_{1n} between ground and QC levels all be equal, so that the Rotating Wave Approximation (RWA) Hamiltonian has the off diagonal elements $H_{1n} = v$.

When the field is sufficiently weak, then only level 2 ever receives appreciable excitation. The population oscillates sinusoidally between level 1 and level 2 with the two-level Rabi period $t_T = \pi/v$. The remaining levels, being far off resonance, do not noticeably participate in the excitation. We can therefore, in first approximation, treat these virtual levels as undergoing independent low-amplitude off-resonant sinusoidal population modulations. Thus the levels nearest to resonance (levels 3 and 4 in Fig. 3) oscillate at the detuned period $\tau = 2\pi/\delta$, the next nearest levels (5 and 6 in Fig. 3) oscillate with period $\tau/2$, and subsequent levels oscillate at $\tau/3$, $\tau/4$, ...etc. The situation is similar to the examples of optical free induction decay (FID) treated by Brewer and Shoemaker[12] and by Foster, Stenholm and Brewer.[13] However, the quasicontinuum differs in an important respect: whereas the FID papers treated the superposed effects of independent two-level atoms, each detuned, we here treat a coupled (N+1)-level system. The distinction can become important.

We see that just as in FID τ constitutes a basic recurrence time.[14] For weak fields the recurrence time is much shorter than the Rabi period. Figure 4, showing plots of level occupation probability P_n for an N = 25-level QC, illustrates this situation: in the first frame we see the sinusoidal Rabi oscillations between levels 1 and 2 as well as the higher-frequency lower-amplitude oscillations into virtual levels 3 and 4. The

long-term (infinite time) population averages P_n show that the virtual levels $n > 2$ have populations some 10^{-3} smaller than the resonant levels 1 and 2.

At the opposite extreme, when the field is sufficiently strong, we can neglect the presence of detuning and treat the system as a degenerate two-level system and the system exhibits periodic depletion of level 1 at the band Rabi period $T_R = t_R/\sqrt{N}$. For such two-level behavior to appear, the bandwidth of the QC levels must be much less than the interaction strength. The first frame of Fig. 5, showing the behavior of populations under this condition, exhibits the expected oscillatory pattern of level 1 populations. Frame 5B shows the expected equalization of long-time population averages amongst QC levels.

In neither of these two extremes is there any obvious behavior indicative of a quasi-continuous distribution of energy levels. The QC becomes evident for intermediate situations, which we next examine.

The condition for weak field excitation is equivalent to the requirement that the recurrence time be much shorter than the two-level Rabi period, $\tau \ll t_R$. Although the population in level 1 gives the appearance of sinusoidal Rabi oscillations, Yeh et al.[11] have shown that the apparent sinusoid actually consists of a piecewise continuous sequence of exponential decays--or linear segments on a semilogarithmic plot of population versus time. The initial decay occurs during the first recurrence time interval $0 < t < \tau$, when the time bandwidth $2\pi/t$ greatly exceeds the detuning. This linear decay occurs according to the traditional Fermi Golden Rule at rate

$$R = 2\pi\rho V^2 = \pi^2\tau/t_R^2 \quad . \tag{1}$$

Here $\rho = 1/\delta$ is the density of energy levels, V^2 is the sum of the individual interaction squares and, as above, t_R is the two-level Rabi period and T_R is the Rabi period appropriate to the full band of levels.

The population does not continue to decay exponentially at rate R indefinitely. What actually occurs is rather curious. During the interval $0 < t < \tau$ the population decays at rate R; during interval $\tau < t < 2\tau$ it decays at rate 3R, etc.[11] Figure 6 illustrates this behavior. This piecewise exponential behavior is quite different from FID. We see here that the piecewise exponential behavior ceases for time exceeding half the two-level Rabi period, $t > t_R/2$. This terminus applies so long as $\tau < t_R/2$. The exponential decay can be prolonged to longer times, up to one Rabi period $t = t_R$, by increasing τ to the value t_R.

As τ ranges over values from $\tau \ll t_R$ to $\tau \gg t_R$ the population histories P_n exhibit a variety of behavior, as shown in Fig. 7. When $\tau \ll t_R$, as is the case for the first frame where $\tau = 2$ and $t_R = 10$, the history of level 1 consists of a very large number of exponential decays, and the curve becomes indistinguishable from a sinusoid. When τ and t_R are approximately equal the exponential decay persists until the time $t = t_R$, after which time the population undergoes near periodic variation. When the recurrence period τ exceeds t_R then the exponential decay curve becomes sinusoidally modulated. Finally when τ greatly exceeds the band Rabi period T_R the behavior shows no sign of exponential decay. Thus for fixed laser power (i.e. fixed t_R) QC behavior is most pronounced for level spacings such that $\tau \cong t_R$ (or $\delta \cong v/2$) and for times $t < \tau$.

Quasicontinuum Propagation

Let us see how the previous treatment of optically thin excitation extends to the treatment of pulse propagation. The same two elementary parameters characterize our study of propagation: the two-level Rabi frequency 2v (i.e., the dipole coupling between level 1 and any one of the QC levels) and the QC level spacing δ. These parameters enter most naturally when regarded as a (two-level) Rabi period $t_R = \pi/v$ and a recurrence time $\tau = 2\pi/\delta$.

We have already mentioned that QC behavior, as manifested by exponential decay of ground-level population, occurs most prominently when these two times are roughly comparable. To exhibit QC behavior most distinctly, we chose values $\tau = 1$ and $t_R = 2$, so that one Rabi period encompassed two recurrence times. Figure 8A shows the population behavior for this choice of parameters, under the assumption of monochromatic excitation starting at $t = 0$. This figure shows quite clearly the exponential decay of level 1 up to time $t = 1 = \tau$. As discussed in the preceding section, the decay rate for conditions of monochromatic excitation is, according to Fermi's Golden Rule, given by Eq. 1 and the population in level 1 follows approximately the decay law

$$P_1(t) = P_1(0)\exp(-Rt) = \exp(-Rt) \tag{2}$$

during the interval $0 < t < 1$.

To examine propagation we assumed a short pulse, of duration much briefer than the repetition time τ (Fig. 8B), so that during the excitation time interval the conditions

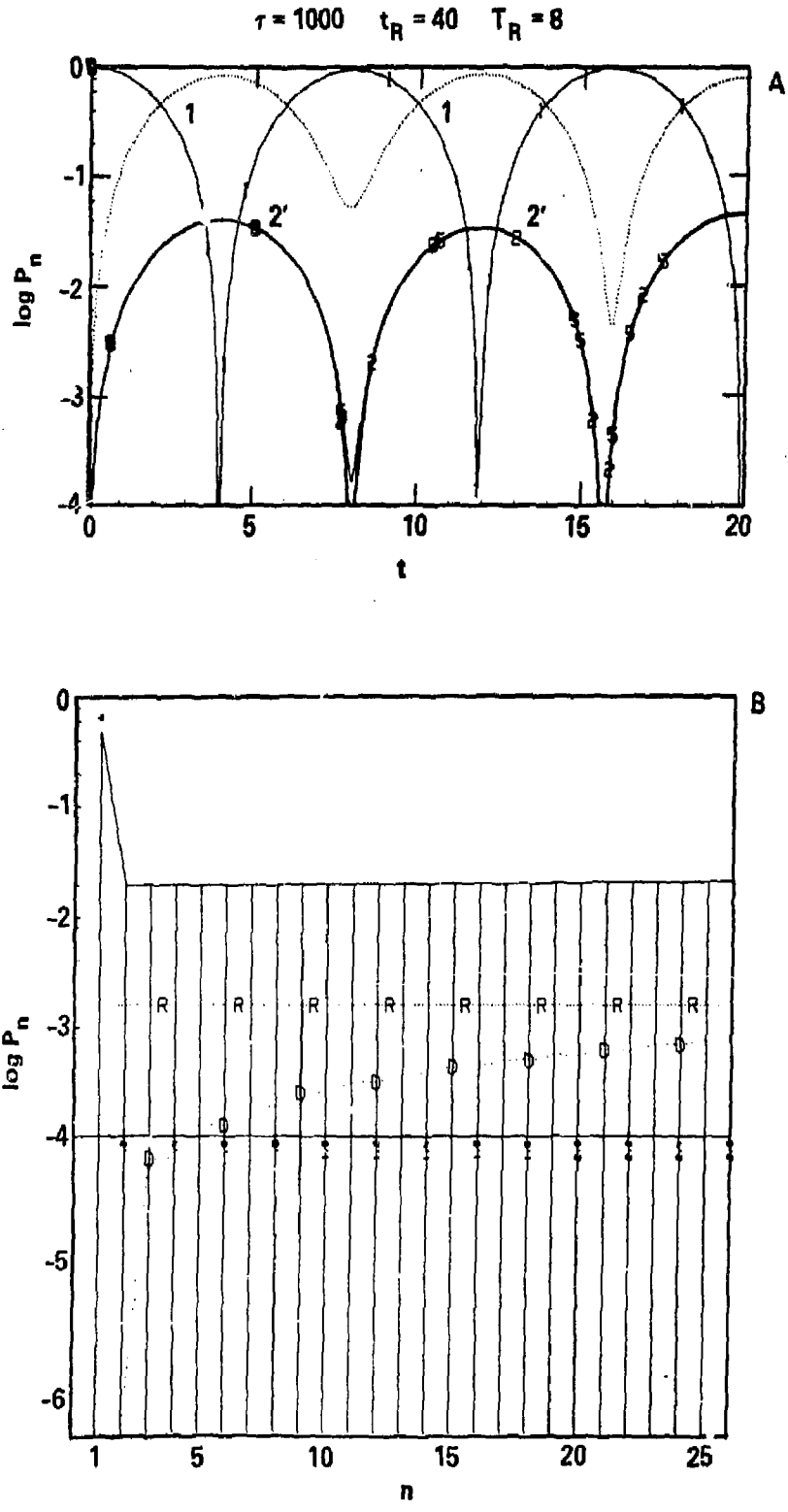

FIG. 5. Strong field quasicontinuum.

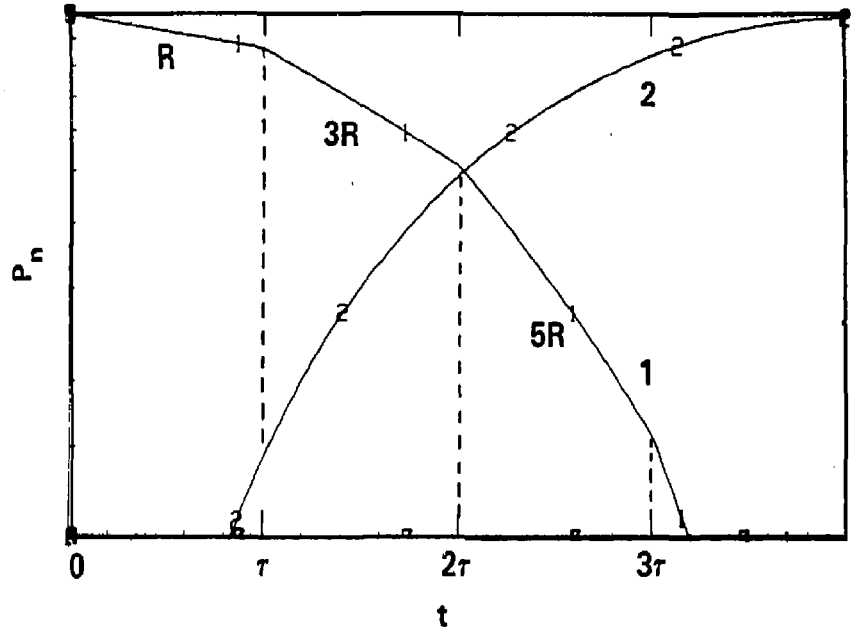

FIG. 6. Quasicontinuum exponential decay.

produce exponential population decay. Figure 8C shows the resulting population variations subject to this pulse.

As this figure shows, once the pulse has passed the molecules at the entry face of the vapor, they remain in a distribution of excited states and hence give rise to a superposition of oscillating dipole moments. In turn these moments act as sources for an electromagnetic field. Each of the QC dipole moments has a different phase, and a frequency fixed by the detuning. At t = 0 these moments are in phase, but after a short time these different phases cancel, so that the total molecular dipole moment vanishes. After one recurrence time these dipoles will again be in phase and hence can produce a total dipole moment. The result is a pulse echo. A second echo occurs after an additional recurrence time. Each such echo produces an impulsive diminution of the excited population by stimulating emission. Figure 8D shows these impulsive changes. They occur cyclically at multiples of the repetition rate.

Figure 9, showing the pulse intensity versus time t and propagation depth z, reveals two recurrence echoes. The initial pulse fluence falls monotonically and in fact satisfies Beer's Law of exponential attenuation.

It is interesting to observe the effect of lengthened repetition time τ upon the pulse echo. Figure 10 shows the echo, obtained with a resonantly tuned N = 7 level QC for a range of recurrence times. In each case the Rabi period $t_R = 2$. For very short recurrence times (e.g., t = 1/4) the echo pattern consists of nearly equidistance pulses. As the recurrence time becomes longer than the pulse duration (e.g., $\tau = 1$) the echo pulses become well separated, and small secondary echoes become visible. These grow with increasing optical depth. As the recurrence time becomes longer than the Rabi period (e.g., $\tau = 4$), and the system consequently approaches 2-level degeneracy, the echo behavior becomes less significant, and we instead observe pulse reshaping. (In all these examples the initial pulse area is 0.2 π, so that soliton formation and self-induced transparency do not occur.)

The echo amplitudes are small compared with the initial pulse; we have therefore used a logarithmic plot to exhibit amplitudes.

It is also interesting to ask: how many levels are sufficient to reproduce the quasicontinuum echo behavior. To answer this question we examined propagation with $t_R = 2$ and $\tau = 1$ for various numbers of QC levels N. Figure 11 shows these results for resonantly tuned excitation (note that with N = 2 and N = 4 the levels are unsymmetrically distributed around the resonant level n = 2). We see that the echo is present as soon as there is a single "outrider" level added to the resonant level (the case N = 2). The addition of further outrider levels (N > 2) steadily sharpens the echo pattern and, in addition, introduces weaker shorter-recurrence echoes.

This behavior alters only slightly when we examine mid-resonant detuning. Furthermore, the primary echoes (those occurring at $t = \tau, 2\tau, 3\tau, \ldots$) are chiefly affected by

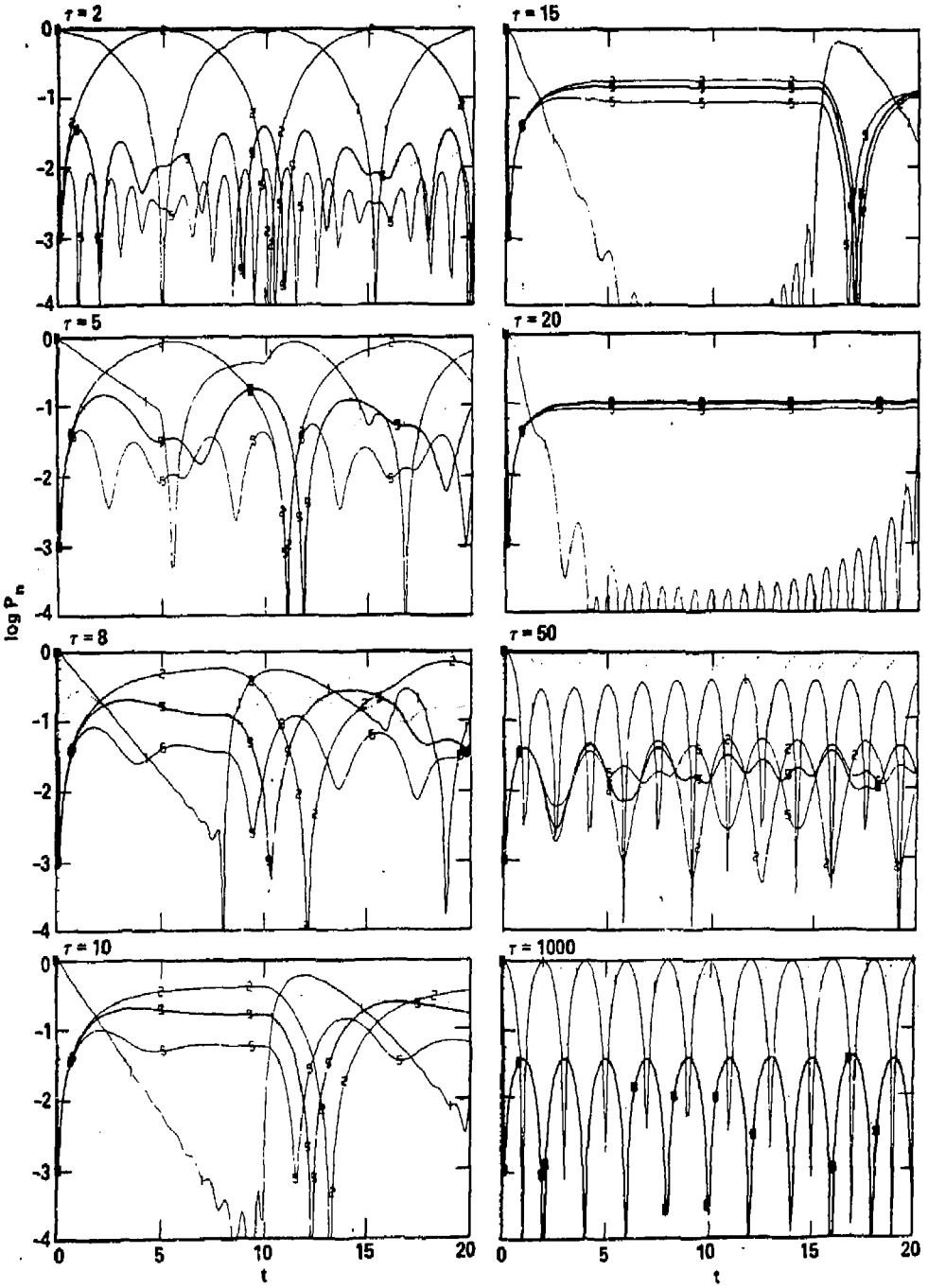

FIG. 7. Quasicontinuum (t_R = 10).

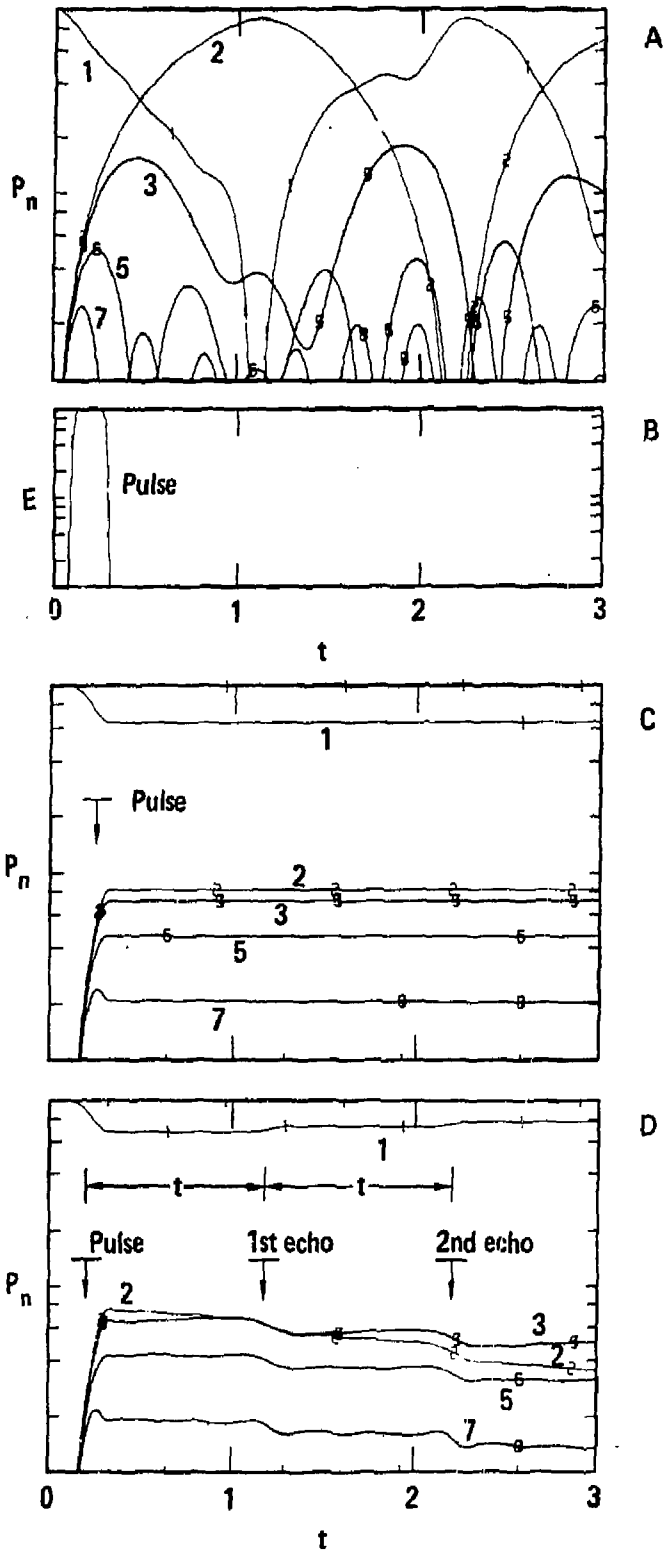

FIG. 8. Quasicontinuum populations, $\tau = 1$ $t_R = 2$.

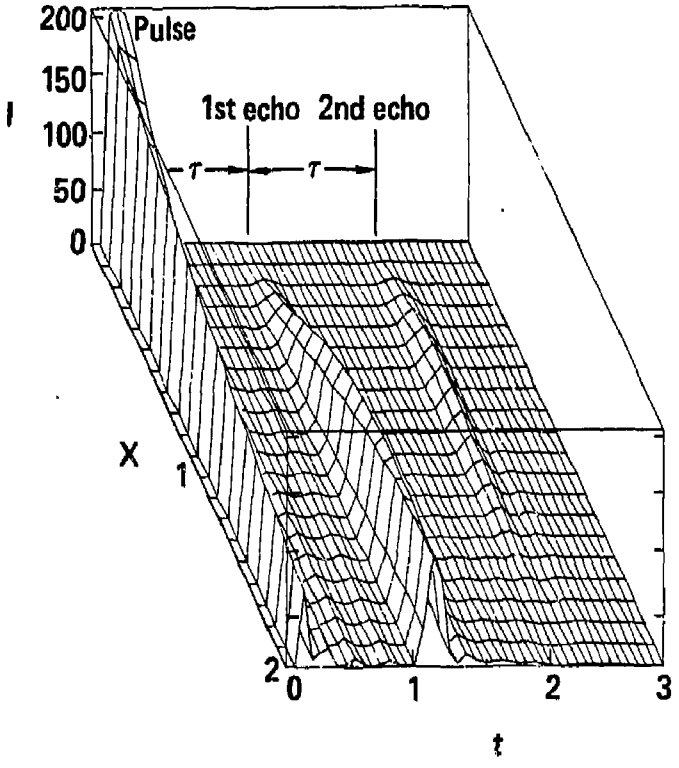

FIG. 9. Pulse intensity, QC model.

the positions of the primary outrider levels (levels 3 and 4 when level 2 is resonant). The spacing of more distance QC levels has little effect upon either the width or the period of the echo pulses, so long as the optical depth remains short enough that secondary echoes do not become dominant. We conclude that quasicontinuum behavior is evidence for as few levels as N = 2.

Conclusions

Our studies, motivated by a desire to understand laser excitation of molecular vapor, have shown particularly interesting phenomena for the example of a molecular quasicontinuum of energy levels. There we observed not only behavior appropriate to an energy continuum (rate-equation excitation and exponential attenuation) but we also observe echo phenomena originating with the discreteness of the energies. The echoes occur after a recurrence time fixed largely by the spacing of the closest outrider levels and are present even in the simplest (N=2) quasicontinuum.

Acknowledgments

We thank Prof. C. D. Cantrell for bringing to our attention the work of Brewer et. al.[12,13] and we thank Dr. R. G. Brewer for correspondence.

This work was performed under the auspices of the U.S. Department of Energy by Lawrence Livermore National Laboratory under Contract W-7405-Eng-48.

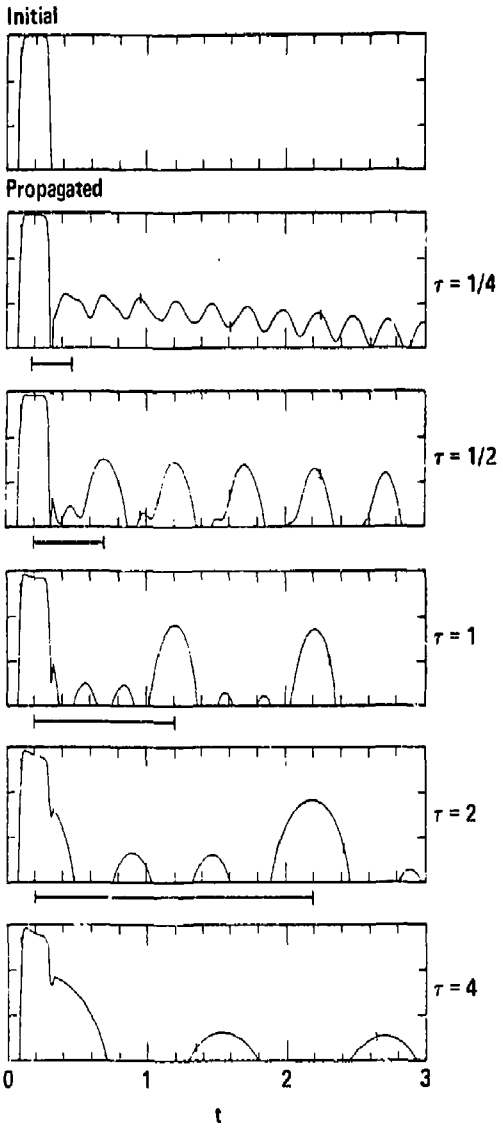

FIG. 10. Resonant QC pulse, $t_{Rabi} = 2$, various τ.

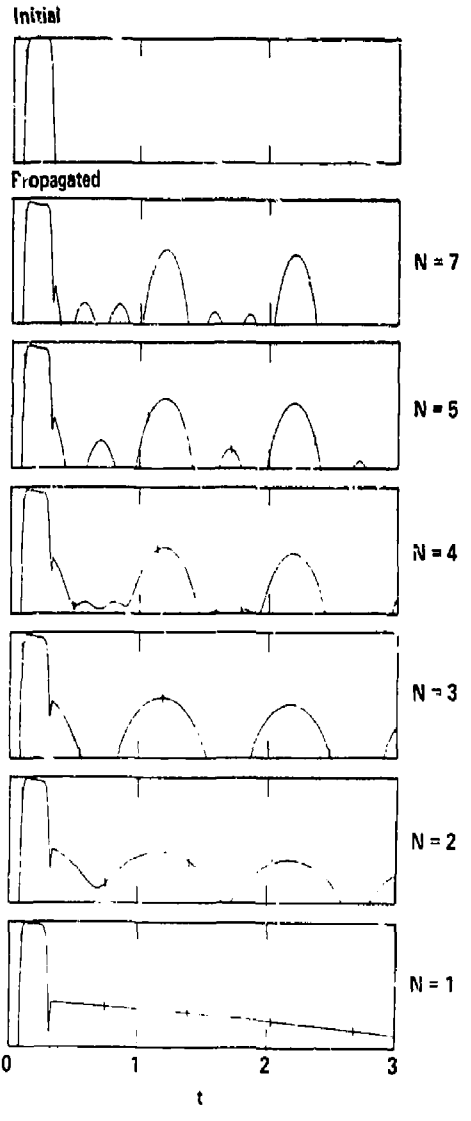

FIG. 11. Resonant QC pulse, $t_{Rabi} = 2$, $\tau = 1$, various N.

References

1. See, for example, L. Allen and J. H. Eberly, Optical Resonance and Two-Level Atoms (Wiley, New York, 1975), Chap. 4.
2. S. L. McCall and E. L. Hahn, Phys. Rev. 183, (1969) 451; G. L. Lamb, Jr., Elements of Soliton Theory (Wiley, New York, 1980), Chap. 7; and Rev. Mod. Phys. 43 (1971) 99.
3. A. A. Makarov, C. D. Cantrell, and W. H. Louisell, Optics Comm. 31, (1979) 31.
4. C. D. Cantrell, F. Rebentrost, and W. H. Louisell, Optics Comm. 36, (1981) 303.
5. G. B. Berman and G. W. Zaslavsky, Physica 2D, (1981) 25.
6. B. W. Shore and J. Ackerhalt, Phys. Rev. A 15, (1977) 1640; J. H. Eberly, B. W. Shore, Z. Bialynicka-Birula, and I. Bialynicki-Birula, Phys. Rev. A 16, (1977) 2038; Z. Bialynicka-Birula, I. Bialynicki-Birula, J. H. Eberly, and B. W. Shore, Phys. Rev. A 16, (1977) 2048; B. W. Shore and J. H. Eberly, Optics Comm. 24, (1978) 83; R. J. Cook and B. W. Shore, Phys. Rev. A 20, (1979) 539; B. W. Shore and R. J. Cook, Phys. Rev. A 20, (1979) 1958.
7. A. Icsevgi and W. E. Lamb, Jr., Phys. Rev. 185, (1979) 517.
8. J. H. Eberly, M. J. Konopnicki, and B. W. Shore, Optics Comm. 35, (1980) 76.
9. B. Segard and B. Macke, Optics Comm. 38, (1981) 96; and B. Macke and F. Rohart, Optica Acta 28, (1981) 1135.
10. M. Quack, J. Chem. Phys. 69, (1978) 1282; A. A. Makarov, V. T. Platonenko, and V. V. Tyakht, Sov. Phys., J.E.T.P. 48, (1978) 1044; C. D. Cantrell, V. S. Letokhov, and A. A. Makarov, in Coherent Nonlinear Optics, edited by M. S. Feld and V. S. Letokhov (Springer, Heidelberg, 1980), Chap. 5.
11. J. J. Yeh, C. M. Bowden, and J. H. Eberly, J. Chem. Phys. (submitted); J. H. Eberly, J. J. Yeh, and C. M. Bowden, Chem. Phys. Letts. (in press 1982).
12. R. G. Brewer and R. L. Shoemaker, Phys. Rev. A 6, (1972) 2001.
13. K. L. Foster, S. Stenholm, and R. G. Brewer, Phys. Rev. A 10, (1974) 2318.